Joint-Channel-Connectivity-Based Feature Selection and Classification on fNIRS for Stress Detection in Decision-Making

Meiyan Huang, Xiaoling Zhang, Xiumei Chen, Yiling Mai, Xiaohua Wu, Jiubo Zhao, and Qianjin Feng, *Member, IEEE*

***Abstract*— Stress is one of the contributing factors affecting decision-making. Therefore, early stress recognition is essential to improve clinicians' decision-making performance. Functional near-infrared spectroscopy (fNIRS) has shown great potential in detecting stress. However, the majority of previous studies only used fNIRS features at the individual level for classification without considering the correlations among channels corresponding to the brain, which may provide distinguishing features. Hence, this study proposes a novel joint-channel-connectivity-based feature selection and classification algorithm for fNIRS to detect stress in decision-making. Specifically, this approach integrates feature selection and classifier modeling into a sparse model, where intra- and inter-channel regularizers are designed to explore potential correlations among channels to obtain discriminating features. In this paper, we simulated the decision-making of medical students under stress through the Trier Social Stress Test and the Balloon Analog Risk Task and recorded their cerebral hemodynamic alterations by fNIRS device. Experimental results illustrated that our method with the accuracy of 0.961 is superior to other machine learning methods. Additionally, the stress correlation and connectivity of brain regions calculated by feature selection have been confirmed in previous studies, which validates the effectiveness of our method and helps optimize the channel settings of fNIRS. This work was the first attempt to utilize a sparse model that simultaneously considers the sparsity of features and the correlation of brain regions for stress detection and obtained an admirable classification performance. Thus, the proposed model might be a useful tool for medical personnel to automatically detect stress in clinical decision-making situations.**

***Index Terms*— Functional near-infrared spectroscopy, stress detection, decision-making, sparse model.**

Manuscript received 18 March 2022; revised 2 June 2022; accepted 1 July 2022. Date of publication 5 July 2022; date of current version 14 July 2022. This work was supported in part by the National Natural Science Foundation of China under Grant 81601562, Grant 81974275, and Grant U1501256; in part by the Science and Technology Planning Project of Guangzhou under Grant 201904010417; in part by the Guangdong Basic and Applied Basic Research Foundation under Grant 2021A1515012011; in part by the Science and Technology Project of Guangdong Province under Grant 2015B010131011; in part by the Special Funds for the Cultivation of Guangdong College Students' Scientific and Technological Innovation under Grant Pdjh2020b0123; and in part by the Ministry of Education in China (MOE) Youth Foundation Project of Humanities and Social Sciences under Grant 2018YJCZH260. *(Corresponding authors: Meiyan Huang; Jiubo Zhao; Qianjin Feng.)*

This work involved human subjects or animals in its research. Approval of all ethical and experimental procedures and protocols was granted by the Ethics Committee of Southern Medical University.

Meiyan Huang and Qianjin Feng are are with the Guangdong Provincial Key Laboratory of Medical Image Processing, with the Guangdong Province Engineering Laboratory for Medical Imaging and Diagnostic Technology, and with the School of Biomedical Engineering, Southern Medical University, Guangzhou 510515, China (e-mail: huangmeiyan16@163.com; fengqj99@smu.edu.cn).

Xiaoling Zhang and Xiumei Chen are with the School of Biomedical Engineering, Southern Medical University, Guangzhou 510515, China (e-mail: zhangxiaoling9911@163.com; chenxiumei97@163.com).

Yiling Mai, Xiaohua Wu, and Jiubo Zhao are with the Guangdong Provincial Key Laboratory of Tropical Disease Research, Department of Psychology, School of Public Health, Southern Medical University, Guangzhou 510515, China, and also with the Department of Psychiatry, Zhujiang Hospital, Southern Medical University, Guangzhou 510515, China (e-mail: maiyiling10@i.smu.edu.cn; wuxh652603@126.com; jiubozhao@126.com).

Digital Object Identifier 10.1109/TNSRE.2022.3188560

I. Introduction

STRESS is regarded as one of the major factors affecting human decision-making. It is a response that an organism produces when stimulated by real or potential threats, accompanied by the psychological experiences of tension and anxiety [1]. Stress has been proved to weaken the goal-oriented ability, increase the habitual behaviors, lead to a more intuitive experience system, and enhance the existing cognitive bias of individuals [2]. Therefore, stress may cause unavoidable consequences in daily life and work, especially in emergency situations. For instance, decision-makers in the medical field, such as doctors, paramedics, and nurses, often make decisions that affect patient morbidity and mortality [3]. Medical staff in high stress situations are more likely to exhibit poor performance compared with people in low stress situations [4], [5]. Fortunately, early cognitive aid for medical staff can be used to reduce the influence of stress on their decision performance. For example, Wetzel *et al.* [6] found that resident trainee surgeons who participated in a "stress management training" course can reduce the stress experienced and improve non-technical skills, including decision-making, in their simulated surgery. Hence, stress detection and management at an early stage may help improve clinicians' decision-making performance.

Stress response is composed of many aspects, such as physiology, psychology, and behavior; thus, stress can be measured from these aspects. Medical questionnaires, such as

the State-Trait Anxiety Inventory [7] and the Perceived Stress Scale [8], generally utilized to assess stress level. Nevertheless, this approach lacks objectivity [9]. In the physiological aspect, stress can activate the sympathetic adrenal medullary system and the hypothalamus–pituitary–adrenocortical axis, which triggers a series of cardiovascular reactions, including increased heart rate (HR), blood pressure (BP), and bioelectricity [10], and leads to the secretion of the cortisol [11]. Cortisol can cross the blood–brain barrier, bind to receptors in the central nervous system, affecting brain function and structure [12]. Therefore, a large number of studies have detected stress by measuring HR variability [6], BP [13], and saliva cortisol levels [14]. However, these methods are influenced by circadian rhythms and cardiovascular diseases [15], [16]. Moreover, salivary cortisol levels is not practical to measure in real time at work. By contrast, evaluating stress by brain signals through electroencephalography (EEG), functional magnetic resonance imaging (fMRI), and functional near-infrared spectroscopy (fNIRS) yields objective and reliable results. fNIRS is a relatively new imaging method in functional neuroimaging research. This imaging modality uses infrared waves in the frequency range of 650–900 nm and then employs the modified Lambert–Beer law to calculate the relative concentration changes of two hemoglobin forms (oxygenated hemoglobin [HbO] and deoxygenated hemoglobin [HbR]). fNIRS can noninvasively detect changes in cerebral blood oxygen levels for a long time; thus, it has a wide range of applications in advanced cognition, developmental psychology, and mental illness in natural situations [17]. fNIRS has better spatial resolution and is less affected by noise than EEG [18] and is more portable and cheaper with less restriction on patients' movement than fMRI, thus, fNIRS is more suitable for the measurement of cerebral blood oxygen in natural situations [19].

The conventional methodology for fNIRS analysis is univariate statistical analysis, which investigates the difference in hemodynamic alterations among different populations by using a single feature of fNIRS signals, such as HbO changes [20]–[23]. For example, Tang *et al*. [22] graded different types of mental stress using the mean HbO value measured by fNIRS during the Montreal Imaging Stress Task, whereas Zhang *et al*. [23] used the same task to reveal the context-dependent response patterns of women to psychosocial stress during dynamic social interactions. Differences between people in stress and nonstress states can be exploited by these methods. However, these methods ignore the underlying hemodynamic features, which may affect the low detection accuracy of stress. Besides, these methods cannot provide a general model to recognize whether a new subject is in stress or not. Thus, multivariate machine learning techniques, which show great promise in disease modeling and therapeutic discovery in psychiatry, have been used as a complement to traditional methods [24]. In previous studies [25]–[27], support vector machine (SVM), linear discriminant analysis (LDA), and decision trees have been applied on fNIRS data to identify specific mental and cognitive tasks for diagnosis or treatment. In the majority of these studies, the statistical characteristics of active channel signals corresponding to the brain region in each trial, such as average, peak, slope, and kurtosis values, can be used as classification features. For instance, Woo *et al*. [25] used LDA to distinguish the difference in fNIRS signals under different stress states with a classification result reaching 76.67%, whereas Park *et al*. [26] used SVM to deal with the same problem and achieved 87% classification accuracy. These results are promising, but exploration by machine learning still has some limitations. For example, the abovementioned methods require feature selection in advance to solve the problem of feature redundancy. Moreover, few studies have considered the relationship among the characteristics of channels corresponding to brain regions. According to previous studies [28]–[30], the human brain is a complex dynamic interactive system. Many brain regions are interconnected in structure and function, and work together to ensure effective information processing and interaction. For this reason, considering the associated brain information may be conducive to the identification of specific cognitive states.

In this paper, we propose a novel joint-channel-connectivity-based feature selection and classification (JCCB-FSC) algorithm for detecting stress in the decision-making process. Notably, the main contributions of this work are three-fold. First, Trier Social Stress Test (TSST) [31] and Balloon Analog Risk Task (BART) [32] are designed as experimental paradigms to simulate the decision-making of medical staff under different stress conditions. Different from the experimental paradigms used in previous studies [22], [23], [25], the proposed paradigms are more in line with the actual state of medical staff's decision-making situation. Second, a sparse model widely used in many studies [33], [34], was applied to simultaneously implement classification and feature selection. Specifically, we devised two regularization terms (intra- and inter-channel regularizers) for the sparse model to explore the potential associations that induce discriminative representations in brain feature space. On the one hand, feature representation is more compact and distinguishable by the intra-channel regularizer. On the other hand, potential correlations among brain regions can be explored by the inter-channel regularizer. Finally, the experimental results show that our proposed method can make accurate predictions and find brain regions highly associated with stress, which helps optimize the channel settings of fNIRS. The proposed method is the first foray into incorporating a sparse model that considers the sparsity of features and the correlation of brain regions simultaneously for stress detection via fNIRS and obtained a great performance. Overall, the proposed model might be used as a potential computer-aided classification tool to perform automatic stress detection for medical staff in the clinical decision-making situation, which may help relieve stress and avoid decision-making errors in time through customized stress training and cognitive aids.

The rest of this article is organized as follows. Section 2 describes the experimental paradigms used in this study and introduces our proposed method in detail. Section 3 presents the experimental results. Sections 4 and 5 provide discussions and conclusion, respectively.

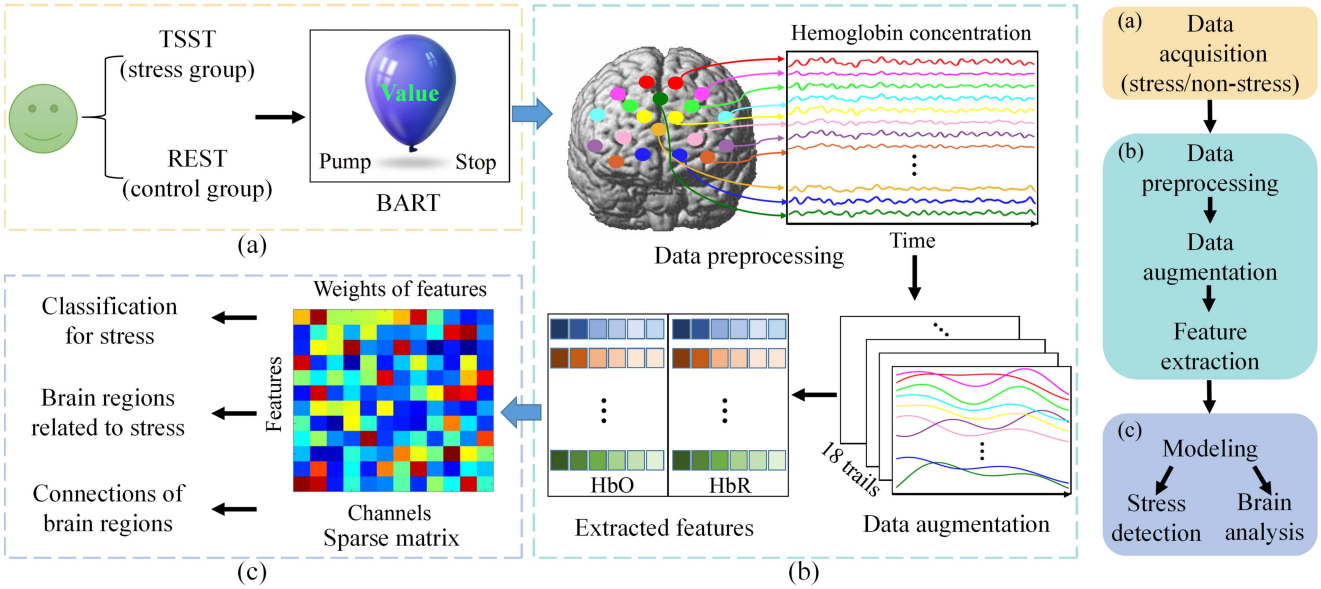

Fig. 1. Flowchart of the proposed framework for stress detection in decision-making. (a) shows the data acquisition process of participants in different groups (stress/control). (b) includes the process of data preprocessing, data augmentation, and feature extraction. (c) displays the modeling of the proposed method for stress detection, and brain analysis.

II. Materials and Method

The proposed method consists of three parts, which are illustrated in Fig. 1. In the first part (Fig. 1 (a)), TSST and BART were designed as experimental paradigms to collect the cerebral hemodynamic signals of participants through fNIRS device. In the second part (Fig. 1 (b)), the obtained fNIRS signals were preprocessed and clipped for data augmentation, and then features were extracted from these signals. In the third part (Fig. 1 (c)), the extracted features were further selected by using JCCB-FSC for stress detection, as well as the stress-associated brain regions and the connections of the detected brain regions.

A. Participants

The participants included 24 healthy college students (6 males, 18 females; age 19-24) who major in medicine and speak Chinese as their mother tongue. Participants with a history of head injury or neurological disorders were excluded. In this study, participants were randomly divided into a stress group (2 male, 10 female) and a control group (4 males, 8 females). Stress was induced by TSST on participants in the stress group. Specifically, we used the Short State Anxiety Inventory (SSAI) [35] and HR recorded by E4 wristband to assist in determining whether the participants are in stress or not. The SSAI and HR of the participants were measured at different time points, including baseline, after TSST/rest (BART beginning), and after BART. Then, the stress-induced effects were determined by repeated-measures analysis of variance (ANOVA). This study was approved by the ethics committee of Southern Medical University. After the study details were fully disclosed, all participants signed the written informed consent. All participants received a certain amount of remuneration in the end of the experiment.

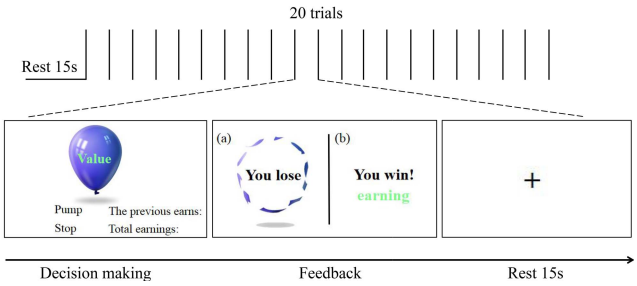

Fig. 2. Experimental process of BART. Twenty trials were conducted, and each trial involved three processes, namely, decision-making, feedback, and rest. In the feedback, (a) and (b) show the negative result and positive results, respectively.

B. Stimuli and Procedure

At the beginning of the study, all participants filled out the SSAI and were informed that they might be asked to participate in a mock interview. However, only participants in the stress group received a detailed description of TSST after completing the questionnaires. They were told that they needed to undergo a job interview without preparation time and their performance was recorded by video. The video was then evaluated by interviewers in the department. Thereafter, the participants would fill out the SSAI again. The nonstress condition group did not receive such instructions but also filled out the form for the second time.

Subsequently, the participants were subjected to a BART experiment. Fig. 2 displays the experimental process of BART. In BART, participants inflate 20 computer-simulated balloons by pressing buttons. A certain amount of money can be earned by each pump. However, the risk of balloon explosion increases as the number of pumps increases. If the balloon explodes, the money earned so far will be lost. Given that decision-making in daily life includes the potential for reward

TABLE I
DISTRIBUTION OF BRAIN REGIONS CORRESPONDING TO EACH CHANNEL

Brodmann area	trainl	Corresponding channel
BA9	Dorsolateral prefrontal cortex (mid-dorsolateral)	2,5,8,9,10,15,17
BA10	Frontopolar area	6,7,12,14,16
BA11	Orbitofrontal area	4, 11, 13, 19
BA46	Dorsolateral prefrontal cortex (ventrolateral)	1,3,18,20

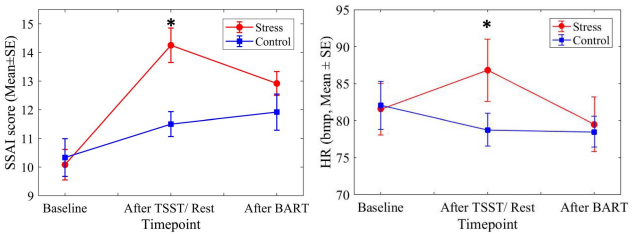

Fig. 3. SSAT scores and HR of subjects in baseline, after TSST (stress group) or rest (control group), and after BART. $*$ indicates that there is significance between the two groups ($p < 0.05$).

and loss [36], this task is an ecologically effective paradigm to simulate adventures under experimental conditions, which can be transferred to risky behavior in real life [37]. At the end of the experiment, participants filled out the SSAI again, and the interviewers answered the questions that the participants wanted to know during the experiment. We recorded the hemodynamic responses of the participants with a continuous wave system (NIRScout) throughout the experiment. To test the effectiveness of stress induction, repeated measures ANOVA was performed on the SSAI and HR. The results showed that the main effect of time ($p = 0.003$) and the main effect of stress ($p = 0.026$) in SSAI, and the main effect of time $\times$ stress ($p = 0.04$) in HR were significant. In addition, as shown in Fig. 3, the SSAI score and HR of the stress group after the end of TSST were significantly higher than that of the control group ($p = 0.006$; $p = 0.036$) whereas there was no significant difference at baseline ($p = 0.814$; $p = 0.596$) and the end of BART ($p = 0.179$; $p = 0.565$).

The NIRScout (NIRx, USA) system with two wavelengths (785 and 830 nm) was used to record cortical hemodynamic changes in the prefrontal cortex area, which is highly correlated with stress [12]. Fig. 4 shows the source and detector array of the fNIRS device and the channel configuration registered to the template of the Brodmann area [38]. The sensor consists of eight dual-wavelength laser diodes and seven detectors to form 20 channels, and the distance between each transmitter and receiver was set to 3 cm at a sampling rate of 7.8125 Hz. The distribution of brain regions corresponding to each channel is listed in Table I.

C. Data Preprocessing and Feature Extraction

The optical intensity time–response curves were preprocessed using nirsLab software provided by NIRScout, where the noise and motion artifacts were eliminated by advanced standard procedures. Channels with a coefficient of variation higher than 7.5% were pruned. A third order band-pass filter with a bandwidth of 0.01–0.2 Hz was designed to reduce noise contamination of the signal. Subsequently, the modified Beer–Lambert law was utilized to convert optical density into HbO and HbR concentrations.

As shown in Fig. 2, each participant underwent 20 trials, and each trial was partitioned into three phases: the decision-making phase (0–10 s, the participants decided whether to inflate the balloon or not), the feedback phase (10–13 s, the participants accepted the result of their decision), and the rest phase (13–28 s, the hemodynamic response returned to baseline). For data augmentation, we divided the data recorded by fNIRS of each participant into 20 independent samples in accordance with trial duration. In each sample, we extracted six statistical features (e.g., average, peak, slope, kurtosis, maximum, and minimum) of two biomarkers (i.e., HbO and HbR) from each channel. Specifically, the statistical features [37], which capture the descriptive information of the signals, were applied to detect stress. Due to the inter-individual variability of signal features, we adopted Z-score normalization to normalize the feature values extracted from each subject to the same scale. In this study, TSST was used as the factor for stress. We labeled the stress and nonstress samples in accordance with whether the participants underwent TSST or not. Although the SSAI scores and HR in the stress group were reduced after BART, previous studies showed that the stress effect induced by TSST would last for a period of time. Specifically, the cortisol level, a specific response to stress, will reach its peak in a period of time (10–30 min) after TSST ends, whereas the subjective scores of stress and HR reach their peak at the end of TSST and then drop to around their baseline after 10 minutes, which are consistent with our measurements (e.g., SSAI and HR). To some extent, stress still exists in BART which lasted 10-15 minutes. Note that we only used the first 18 trials of each participant's data in consideration of the subside effect of stress. Finally, we obtained a dataset with a sample size of 432 (i.e., 24 subjects and 18 trials in each subject: $24 \times 18 = 432$) and 240 extracted features in each sample (i.e., 20 channels and 6 features of HbO and HbR signals in each channel, respectively: $20 \times 6 \times 2 = 240$).

D. JCCB-FSC

Herein, bold capital letters can be used to denote matrices, and bold lowercase letters can be assigned to vectors. In particular, we arranged the fNIRS feature vectors in a matrix $\mathbf{X} \in \mathrm{R}^{q \times n}$ and their respective label (the task version performed by

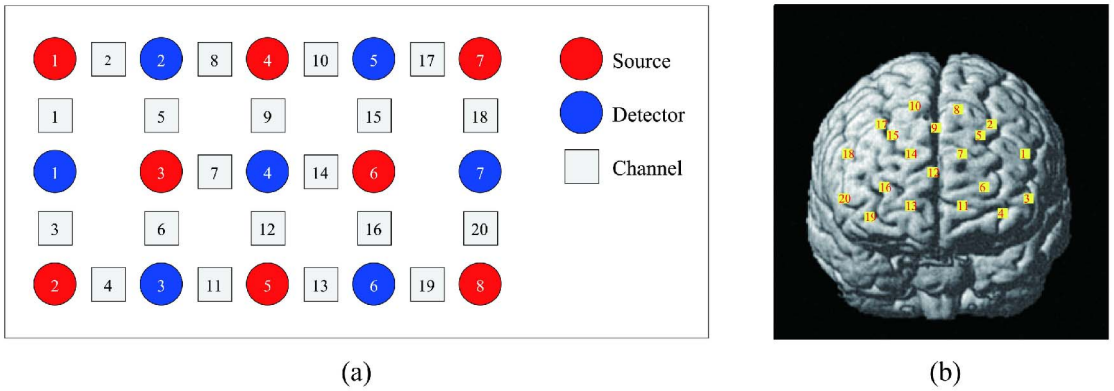

Fig. 4. Optode placement and channel configuration of fNIRS device. (a) shows the source and detector array of fNIRS device, and (b) shows channel distribution registered to the brain.

participants, stress or nonstress) in $\mathbf{y} \in \mathrm{R}^n$, where q and n are the feature dimension and number of samples, respectively. In addition, $\|\mathbf{X}\|_2^2 = \sum_i \sum_j x_{ij}^2$ and $\|\mathbf{X}\|_1 = \sum_i \sum_j |x_{ij}|$ represent l_2 and l_1 norms of $\mathbf{X}$, respectively, where x_{ij} denotes the elements in the i-th row and j-th column of the matrix $\mathbf{X}$.

1) Sparse Feature Selection Model: Feature selection refers to the process of selecting a subset of distinguishing features from the original features to best construct a model for classification or regression. Among the feature selection methods, sparse feature selection [39] with simplicity and superior performance has attracted widespread attention in recent years.

Sparse feature selection in this study aims to minimize the following goals to obtain a representation of the samples using the best weight vector $\mathbf{w} \in \mathrm{R}^q$:

$$\min_{\mathbf{w}} \left\| \mathbf{y} - \mathbf{w}^T \mathbf{X} \right\|_2^2 + \lambda \|\mathbf{w}\|_1 \tag{1}$$

This weight vector is constrained by l_1 norm to obtain a compact set of discriminative features. However, the data distribution must be assumed in advance during the process of linear regression; in many cases, the assumed distribution is inaccurate. Moreover, the associated information among brain regions is discarded in (1).

2) Object Function: In order to build a more flexible and robust model, we propose a joint-channel-connectivity-based feature selection and classification algorithm. The object function is expressed as follows:

$$\min_{\mathbf{w}} \sum_{i=1}^{n} (-y_i \mathbf{w}^T \mathbf{x}_i + \ln(1 + e^{\mathbf{w}^T \mathbf{x}_i})) + \lambda_1 \|\mathbf{w}\|_1 + \lambda_2 \|\mathbf{w}\|_{2,1} + \lambda_3 \mathbf{w}^T \mathbf{L} \mathbf{w}. \tag{2}$$

To solve the limitation of a simple linear model, we used a logistic function $\mathbf{y} = \frac{1}{1+e^{-\mathbf{w}^T \mathbf{X}}}$ to connect the true label $\mathbf{y}$ of the classification task with the predicted value of the linear regression model, and then estimated $\mathbf{w}$ through the maximum likelihood method. Given that fNIRS data were collected by multiple channels, some potential group structure information of channels were ignored by (1). To address this issue, we added a l_{21} norm denoted by (3) to make the feature representation more compact by considering the group information of channels. In (3), 20 groups (channels) were included, and each group has a weight vector corresponding to the 12 features of each channel. Therefore, the l_{21} norm enforces group-wise sparsity, which indicates that features at the group level will be selected or unselected simultaneously.

$$\|\mathbf{W}\|_{2,1} = \sum_i \|\mathbf{w}_i\|_2 = \sum_i \sqrt{\sum_j w_{ij}^2} \tag{3}$$

Furthermore, taking association information among brain regions into consideration, we introduced a connection-based penalty item [33], which is formulated as follows:

$$P(\mathbf{w}) = \mathbf{w}^T \mathbf{L} \mathbf{w} \tag{4}$$

where $\mathbf{L}$ is the Laplacian matrix of the connection matrix of fNIRS features. The Laplacian matrix is defined as $\mathbf{L} = \mathbf{D} - \mathbf{C}$, where $\mathbf{C}$ is the connection matrix of fNIRS features, and $\mathbf{D}$ is the degree matrix of matrix $\mathbf{C}$. Each element of $\mathbf{C} \in \mathrm{R}^{q \times q}$ is calculated by (5).

$$C_{kl} = \begin{cases} \left[\dfrac{\sum_{i=1}^{n} (x_{ik} - \overline{x_k})(x_{il} - \overline{x_l})}{\sqrt{\sum_{i=1}^{n} (x_{ik} - \overline{x_k}) \sum_{i=1}^{n} (x_{il} - \overline{x_l})}} \right]^2, & k \neq l \\ 0, & k_1 = l \end{cases} \quad k, l = 1, 2, \ldots, q \tag{5}$$

In conclusion, feature sparsity at the individual level and group level, and the potential information of brain connectivity are incorporated into the proposed method. Therefore, features that play an important role in the classification task can be detected by (2).

3) Optimization Algorithm: The minimum of the loss function should be obtained to effectively solve the problem of formula (2). The loss function can be defined as:

$$\mathcal{L}(\mathbf{w}) = \sum_{i=1}^{n} (-y_i \mathbf{w}^T \mathbf{x}_i + \ln(1 + e^{\mathbf{w}^T \mathbf{x}_i})) + \lambda_1 \|\mathbf{w}\|_1 + \lambda_2 \|\mathbf{w}\|_{2,1} + \lambda_3 \mathbf{w}^T \mathbf{L} \mathbf{w}. \tag{6}$$

To find the minimum of (6), the gradient descent method was applied to update the variables. Specifically, we calculated the derivative of the loss function with respect to $\mathbf{w}$ as follows:

$$\frac{\partial \mathcal{L}(\mathbf{w})}{\partial \mathbf{w}} = -\sum_{i=1}^{n} \mathbf{x}_i \left(y_i - \frac{e^{\mathbf{w}^T \mathbf{x}_i}}{1 + e^{\mathbf{w}^T \mathbf{x}_i}}\right) + \lambda_1 \mathbf{D}_1 \mathbf{w} + \lambda_2 \mathbf{D}_2 \mathbf{w} + 2\lambda_3 \mathbf{L}\mathbf{w}. \quad (7)$$

In (7), $\mathbf{D}_1 \in \mathrm{R}^{q \times q}$ is a diagonal matrix, in which the i-th diagonal element is$1/\left\|w_{m,i}\right\|_2$, where m represents the corresponding channel. $\mathbf{D}_2 \in \mathrm{R}^{q \times q}$ is also a diagonal matrix, of which i-th diagonal element is $1/\|w_i\|_2$. The iteration formula of $\mathbf{w}$ is

$$\mathbf{w}^{k+1} = \mathbf{w}^{k+1} - \alpha \frac{\partial \mathcal{L}(\mathbf{w}^k)}{\partial \mathbf{w}^k} \quad (8)$$

where α represents the search step in the gradient direction. When $\mathcal{L}(\mathbf{w}^{k+1}) - \mathcal{L}(\mathbf{w}) < 10^{-5}$, the iteration will be stopped, and the final optimized weight $\mathbf{w}$ will be obtained.

III. Experiment Results

In this section, we compared the performance of stress and control groups in BART and then quantified the performance of our algorithm by detecting stress in decision-making. For stress detection, we first adjusted parameters of the model, and then we verified the role of each regularizer in JCCB-FSC. Subsequently, we compared our approach with various machine learning methods such as k-nearest neighbor (KNN), LDA, SVM, and random forest (RF). In particular, two feature selection techniques based on mutual information (MI) and Relief-F [40], [41] were applied before the four comparison methods, respectively. All methods, including the comparison methods and ours, used the same strategy for parameter tuning and model training. Finally, the effectiveness of feature selection would be validated. A nested 10-fold cross-validation strategy was applied for the evaluation of the proposed method. Specifically, for the external loop, we divided the dataset into 10 similarly sized subsets through hierarchical sampling. In each run, samples in a subset were selected successively as the test set, while the remaining subsets were combined as the training set for model training and parameter tuning. The final results were obtained from the mean results of each run. For the inner loop, the training set was further divided into training and validation parts. The proposed method with different parameter values can be trained in the training part, and the parameters with optimized mean results in the validation part were selected to obtain the optimized model for testing. Similarly, the comparison methods used the same strategy to obtain the optimal feature subset and the optimal model in the training set, and further evaluated the performance of the model in the test set. Given that each participant has 18 trials, we split different subsets in accordance with participants to prevent overestimating different methods. For example, 22 subjects were in the training set and two subjects were in the test set, so the sample sizes of the training and test sets were 396 ($22 \times 18 = 396$) and 36 ($2 \times 18 = 36$), respectively. Accuracy was used as measurements during the process. The code of JCCB-FSC is available at the code sharing site (https://github.com/Meiyan88/JCCB-FSC).

A. Results From Behavioral Measure

According to previous studies [42], [43], we computed the mean and standard deviation of BART behavioral data (i.e., the total number of "wins" and "losses", average adjusted inflations per "win" and "lose" balloons, and total earnings). Additionally, tests of normality (Kolmogorov-Smirnov tests) were conducted on BART behavioral data. The differences between the two groups were assessed using one-way ANOVA on normally distributed behavioral data and independent samples Mann–Whitney U test for non-normal data. Total and group-specific (stress/control group) BART descriptive data are presented in Table II. All behavioral data were normally distributed except the average adjusted inflation "win" balloon, for which stress differences were calculated in their corresponding way, as noted in Table II. There were no statistically significant stress differences in the number of "win" or "lose" balloons ($p = 0.10$). However, compared with the stress group, the control group did perform significantly more balloon inflations which led to a win ($U = 34.0$; $z = -2.18$; $p = 0.03$). Although there was no significant stress difference in the number of total earnings ($p = 0.44$), the statistical results also showed that the control group made more money than the stress group (control group: 86.79 ± 32.33; stress group: 73.58 ± 60.95).

B. Parameters Selection

In the JCCB-FSC model, three parameters, namely, λ_1, λ_2, and λ_3, were designed to control the trade-off between the sparsity of feature selection and the degree of connectivity contribution of brain regions, which would be optimized within the internal loop in the training set. To evaluate the effects of λ_1, λ_2, and λ_3 on the performance of JCCB-FSC, we tuned the optimal parameters through grid search from the following finite set: [10^{-5}, 10^{-4}, 10^{-3}, 10^{-2}, 10^{-1}, 10^{0}, 10^{1}]. Fig. 5 shows the accuracy result of different parameter sets, where we found that the best λ_1, λ_2, and λ_3 falls in the range of [10^{-4}, 10^{-3}], [10^{-2}, 10^{-1}], and [10^{-4}, 10^{-2}], respectively. Then, final results of test set were obtained by using the optimal parameters.

C. Ablation Experiments

To verify the effect of each regular term, we removed one regular term at a time to observe the changes in the performance of the entire model. Table III shows that the accuracy of stress detection during decision-making slightly decreased when one of the regular terms was removed. In particular, when the connectivity-based penalty was removed, the accuracy of JCCB-FSC decreased more obviously, indicating the importance of considering connectivity of brain regions.

D. Comparison With Other Methods

To evaluate the proposed method, we compared the performance of the JCCB-FSC model with four competitive machine learning techniques, (i.e., KNN, LDA, SVM, and RF). Table IV displays the classification performance. We found that the proposed method attained the highest classification

TABLE II
BART BEHAVIORAL DATA

Behavioral data	Total group (n = 24)	Control group (n = 12)	Stress group (n = 12)	Group difference
Number of "win" balloons	9.29 ± 2.36	8.50 ±1.78	10.08 ± 2.68	F = 2.91, p^a = 0.10
Number of "lose" balloons	10.71 ± 2.36	1.5 ± 1.78	9.92 ± 2.68	F = 2.91, p^a = 0.10
Average adjusted inflations /"win" balloon	6.25 ± 1.49	6.93 ± 0.88	5.46 ± 1.72	**U = 34.0, z = -2.18, p^b = 0.03**
Average adjusted inflations /"lose" balloon	4.34 ± 0.52	4.41 ± 0.49	4.27 ± 0.56	F = 0.43, p^a = 0.52
Total earnings	80.19 ± 48.19	86.79 ± 32.33	73.58 ± 60.95	F = 0.44, p^a = 0.51

[a] One-way ANOVA.
[b] Nonparametric independent samples Mann–Whitney U test.
n is the number of the participants.

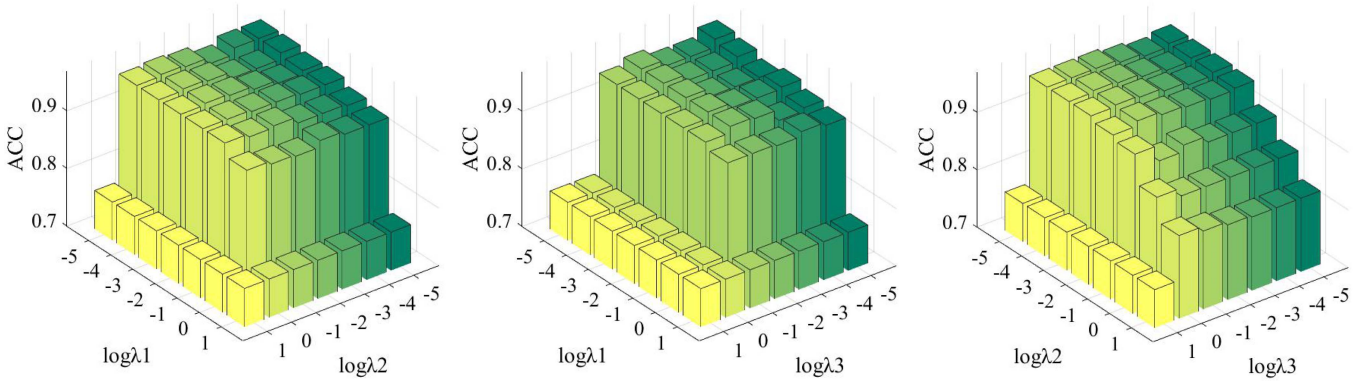

Fig. 5. ACC results of different parameter settings.

TABLE III
STRESS DETECTION ACC OF JCCB-FSC IN ABLATION EXPERIMENTS

l_1 norm	l_{21} norm	connectivity-based penalty	ACC
--	√	√	0.950±0.045
√	--	√	0.956±0.048
√	√	--	0.944±0.052
√	√	√	0.961±0.044

accuracy (0.961 ± 0.044) among all methods. This finding showed that considering the associated information of brain regions and making the feature representation more compact may be more conducive to identifying specific cognitive states. Between the two feature selection methods applied to our dataset, the feature subset selected by the Relief-F algorithm was more suitable for KNN and LDA, whereas the feature subset selected by the MI-based algorithm was more suitable for SVM and RF. Moreover, a paired-sample t-test was applied to further explore the difference among these results. The results showed that the proposed method was significantly different ($p < 0.05$) from other methods, except for RF with feature selection based on MI. A potential reason for the performance of RF is that RF is an ensemble machine learning method with a structure of optimal subset partition. The diversity of base learners of RF comes not only from sample disturbances but also from attribute disturbances, which leads to the generalization performance of the ensemble being further improved by the increase in differences between individual learners [44], [45].

E. Feature Selection

In this section, we first investigated whether statistically significant differences exist in hemodynamic activity during decision-making under different stress states, and compared the statistical results with our method in feature selection. Subsequently, the connectivity of brain regions was explored.

As shown in Figs. 6(a) and (b), a paired-sample t-test showed a significant difference between stress state and non-stress state ($p < 0.05$). Compared with the hemodynamic response during decision-making in nonstress state, HbO changes under stress were significantly higher in channels 4, 11, 13, and 18, whereas HbR changes were in suppression in channels 3, 4, 9, 10, and 17. In this study, we not only detected stress in decision-making but also selected features related to stress. Fig. 6(c) displays the weight amplitude of features, where the brighter the color is, the more important the feature is. Additionally, we sorted out the mean weight of each channel, and then found that the higher feature weights were concentrated in the channels 3, 4, 7, 13, 14, 17, 18, 19, and 20. These results were roughly similar to the findings of paired-sample t-test which could be used to prove the effectiveness of feature selection of our method. Furthermore, we used features of the selected channels for classification, and also achieved a good accuracy of 0.953 ± 0.037, which illustrated the possibility of using fewer fNIRS channel settings to achieve good pressure prediction results.

According to the previous studies [28]–[30], different parts of the brain work together to ensure effective information processing and interaction. Therefore, in the process of detecting stress, we took into account the potential correlations

TABLE IV

CLASSIFICATION RESULTS OF DIFFERENT METHODS. RELIEF-F AND MI-BASED FEATURE SELECTION METHODS WERE ONLY APPLIED TO THE COMPARISON METHODS. THE HIGHEST VALUES AMONG THE RESULTS FROM THE FIRST AND THIRD ROWS ARE SHOWN IN BOLD. *p*-VALUES OF PAIR-SAMPLES *t*-TEST COMPARING THE DIFFERENT METHODS WITH THE PROPOSED METHOD ARE LISTED IN THE SECOND AND FOURTH ROWS

Method		SVM	RF	KNN	LDA	JCCB-FSC
Relief-F	Accuracy	0.887 ± 0.082	0.918 ± 0.055	0.875 ± 0.060	0.879 ± 0.077	**0.961 ± 0.044**
	p	0.0079	0.0485	0.0045	0.0084	--
MI-based method	Accuracy	0.919 ± 0.086	0.925 ± 0.047	0.873 ± 0.078	0.881 ± 0.073	**0.961 ± 0.044**
	p	0.0167	0.0768	0.0020	0.0071	--

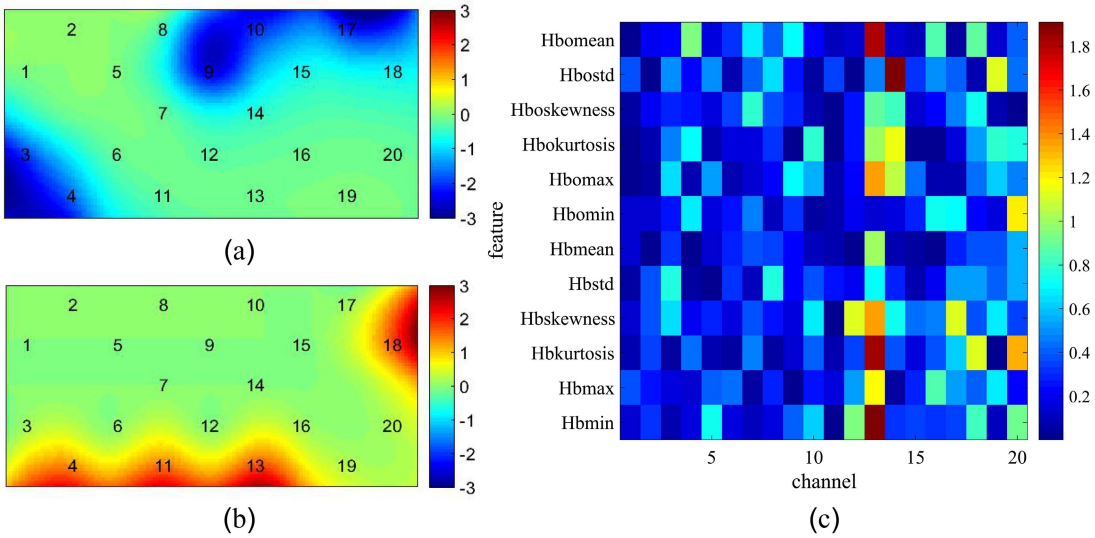

Fig. 6. Results of group differences in hemodynamic activity and feature selection. (a) and (b) show the *t*-test results of HbR and HbO ($p < 0.05$), respectively. The blue area indicates lower activation in the stress group during decision-making and the red area indicates higher activation. (c) shows the weight amplitude of features calculated using the proposed method.

among channels. To verify the effectiveness of our method, we calculated the Pearson's correlation of weights obtained by the proposed method. It is worth noting that we calculated the average weight of 10-fold cross-validation as the functional connectivity (FC) value to obtain a robust result. Moreover, the FC matrixes of the stress and control groups were calculated, and the difference in connectivity strength between the stress and control groups was explored by *t*-test. The results are shown in Fig. 7. Figs. 7(a), (b), and (c) represent the total, stress, and control groups, respectively. In the figures, the yellow area indicates a more active node, which shows that it has a higher relevance or synchronization level, and the green area indicates a lower degree of relevance between channels. Figs. 7(b) and (c) show that the yellow area for the stress group is larger than that for the control group. In Fig. 7(d), the blue area shows the obvious difference in the FC matrixes of the two groups (stress and control groups, $p < 0.05$), whereas the red boxes are the areas of significant correlation in Fig 7(a) ($p < 0.05$). Some overlap between the blue area and red boxes in Fig. 7(d) was found: Ch1–Ch11, Ch3–Ch8, Ch5–Ch15, Ch8–Ch11, and Ch13–Ch18. Moreover, we utilized the BrainNet Viewer toolkit [46] for visualization of the overlap areas. From Fig. 7(e), most of the connections were concentrated in the orbitofrontal area, ventrolateral prefrontal cortex, and mid-dorsolateral prefrontal cortex. These findings were consistent with those of previous studies on decision-making under stress [47]–[49], which also demonstrated that brain connectivity can provide useful information for detecting stress in decision-making.

IV. DISCUSSIONS

A. Effect of Regularizers

In this article, we conducted an ablation experiment to verify the role of each regular term on the proposed method. Table III shows that the performance of JCCB-FSC was attenuated to a certain extent each time a regular term was eliminated. Specifically, the accuracy of JCCB-FSC decreased more significantly when the connectivity-based penalty was removed. These results indicated that group information of channels and correlations among channels play an important role in analyzing cerebral hemodynamic alterations of the brain when performing specific cognitive tasks, and they should be considered when analyzing fNIRS data.

B. Comparison With Previous Studies

We compared JCCB-FSC with four other commonly used machine learning methods for fNIRS data analysis. Table IV

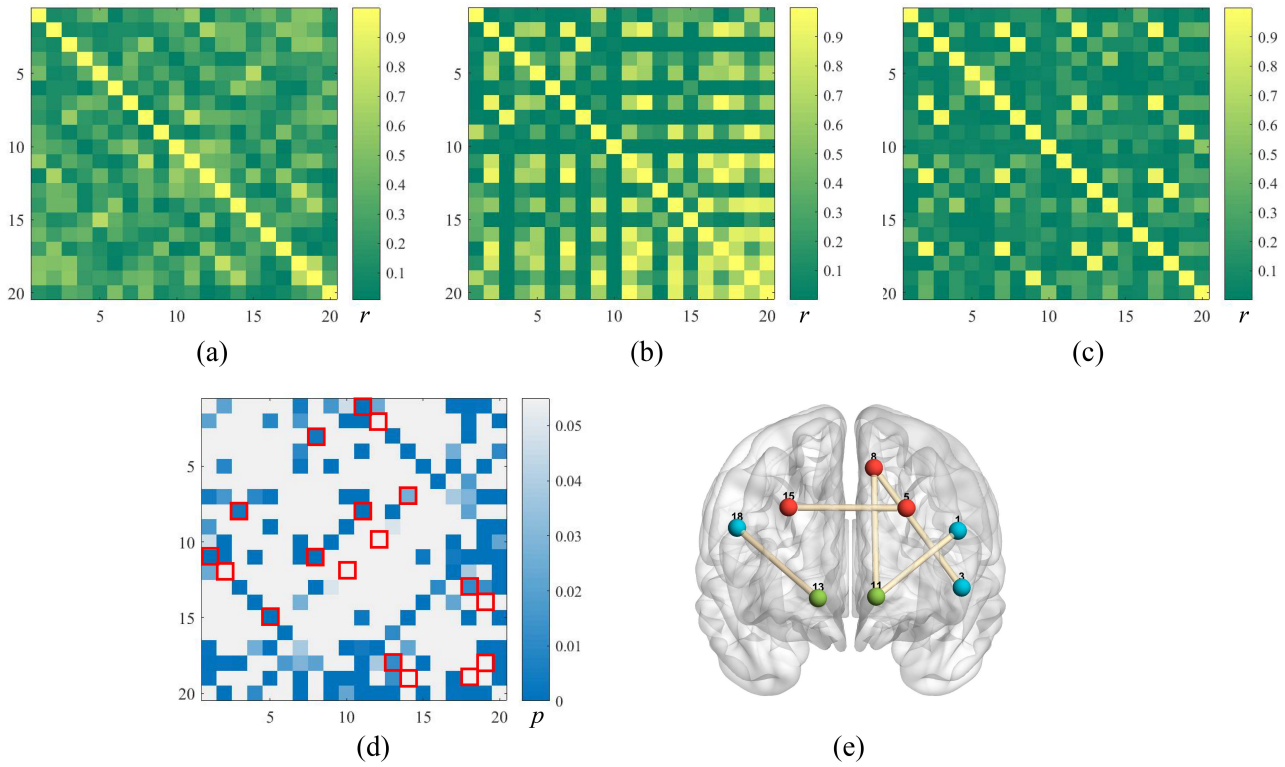

Fig. 7. Results of functional connectivity patterns. (a) shows the FC matrix calculated by the average weight of 12 features (e.g., average, peak, slope, kurtosis, maximum, and minimum of HbO and HbR). (b) and (c) show the FC matrixes of the stress and control groups, respectively. (d) presents the difference in connectivity strength between the two groups by *t*-test ($p < 0.05$), where the blue area indicates a significant difference between the groups, and the red boxes are the areas of significant correlation in Fig 7(a) ($p < 0.05$). (e) presents the brain connectivity pattern of overlap between the blue area and red boxes in (d), where the point colors of red, green, and blue symbolize the mid-dorsolateral prefrontal cortex, orbitofrontal area, and ventrolateral dorsolateral prefrontal cortex, respectively.

shows that JCCB-FSC achieved the highest accuracy (0.961 ± 0.044) among the comparison methods. The results of paired-sample *t*-test also proved that the performance of JCCB-FSC was better than most of the comparison methods, except for RF with feature selection based on MI. For stress detection in decision-making, the reason why our method demonstrated better performance was that it considered the sparsity of fNIRS features and potential associated information of channels in analyzing fNIRS data. Moreover, the proposed method was a combination of feature selection and classification, whereas the comparison methods required additional feature selection strategies. These results indicated that JCCB-FSC is more flexible in detecting stress in the decision-making process.

To further verify the robustness of the proposed method, the proposed method was performed separately on two publicly available datasets. One of the available datasets [50] were collected from 10 healthy subjects and 18 stroke patients by using a portable NIRSIT device (OBELAB, Korea), which had been preprocessed and can be available at https://data.mendeley.com/datasets/6mbzffznr6/. Another dataset were collected from 21 healthy adults by using a CW7 NIRS system (TechEn Inc. MA, USA), which were raw data recording the cerebral hemodynamic alterations of subjects during observed versus executed motor tasks. The dataset can be available at https://www.nitrc.org/projects/li20mirror/, and the fNIRS data were preprocessed using Homer2 software [51], and more details on the data analysis of this dataset can be found in [52]. Briefly, data pretreatment, data augmentation, feature extraction, and feature selection were conducted on both publicly available datasets, and then the JCCB-FSC model and four comparison methods were applied to both datasets. Table V shows the classification results of the above datasets. The classification accuracy of the proposed method reached 0.940 ± 0.039 in the first public dataset and 0.724 ± 0.054 in the second dataset. The difference in classification performance between the two datasets might be caused by the differences in experimental paradigm and task specification standards [53]–[55]. However, for both publicly available datasets, our approach achieved the highest classification accuracy in comparison with the four other methods. The improvements in JCCB-FSC may be from the intra- and inter-channel regularization terms that take full advantage of the potential associated information of channels. These results also proved the applicability of our method to different datasets.

C. Feature Selection

In addition to detecting stress in decision-making, we are still interested in the features and channels of fNIRS related to stress. Based on (6), three regular terms constrain the feature representation. When the calculated feature weight is higher, the corresponding feature is more important, and vice versa. Fig. 6(c) shows the feature weight amplitude map obtained

TABLE V

CLASSIFICATION RESULTS OF DIFFERENT METHODS ON TWO PUBLICLY AVAILABLE DATASETS. RELIEF-F AND MI-BASED FEATURE SELECTION METHODS WERE ONLY APPLIED TO THE COMPARISON METHODS. THE HIGHEST VALUES AMONG THE RESULTS FROM THE FIRST AND THIRD ROWS ARE SHOWN IN BOLD. *p*-VALUES OF PAIRED-SAMPLE *t*-TESTS COMPARING THE DIFFERENT METHODS WITH THE PROPOSED METHOD ARE LISTED IN THE SECOND, FOURTH, SIXTHE, AND EIGHTH ROWS

	Method		SVM	RF	KNN	LDA	JCCB-FSC
Dataset 1 (normal and stroke)	Relief-F	Accuracy	0.838 ± 0.046	0.872 ± 0.061	0.901 ± 0.055	0.898 ± 0.063	**0.940 ± 0.039**
		p	0.0003	0.0157	0.0472	0.0274	--
	MI-based method	Accuracy	0.858 ± 0.028	0.873 ± 0.061	0.906 ± 0.034	0.907 ± 0.038	**0.940 ± 0.039**
		p	0.0010	0.0021	0.0213	0.0178	--
Dataset 2 (observed and executed)	Relief-F	Accuracy	0.720 ± 0.060	0.669 ± 0.041	0.657 ± 0.059	0.663 ± 0.059	**0.724 ± 0.054**
		p	0.2768	0.0273	0.0216	0.0226	--
	MI-based method	Accuracy	0.699 ± 0.030	0.675 ± 0.041	0.675 ± 0.053	0.669 ± 0.049	**0.724 ± 0.054**
		p	0.0946	0.0123	0.0183	0.0156	--

by the model. The brighter the color, the important the weight of the feature, and the more relevant the hemodynamic response under pressure. Besides, we also sorted the average feature weights of the 20 channels on the collected fNIRS data, and the top nine channels were selected to compare with the paired sample *t*-test results of the hemodynamic response (Figs. 6 (a) and (b)). The comparison results showed that channels selected by the above two methods had a large overlap, which shows the effectiveness of JCCB-FSC feature selection. Most of these selected channels were concentrated in the dorsolateral prefrontal cortex and frontopolar area which are essential for developing an appropriate response to environmental changes [56]. These brain regions contain a large number of receptors for stress hormones (e.g., cortisol). By causing the release of cortisol, stress alters the neural activities of these brain regions, further affecting behaviors [57], [58]. Furthermore, we explored the brain connectivity in decision-making under stress. Specifically, the average weight of 10-fold cross-validation was used to calculate the contribution index of FC (Fig. 7(a)), and Fig. 7(e) displays the brain connectivity pattern of the overlap of significant connection ($p < 0.05$) between the condition difference and the total significant correlations. Some brain regions, including the dorsolateral prefrontal cortex and frontopolar area, have strong connectivity. As described in [57], BA9, BA10, and BA11 in Table I constitute the prefrontal cortex associated with working memory, emotions, and perform cognitive functions together, which are related to stress in decision-making. In summary, the feature selection achieved by our method has certain significance for optimizing channel settings of fNIRS and providing a direction for exploring brain connectivity under stress.

D. Limitations and Future Work

In this research, we found that JCCB-FSC showed a great improvement over other machine learning methods, but several issues still need to be resolved in future work. First, factors such as the subject's gender or personality characteristics may interact with stress in decision-making [59], which is likely to have an influence on our research findings. Since these factors were not considered during the recruitment of volunteers, future studies should address these factors as potential exclusion factors or control factors. Second, the datasets used in previous studies of fNIRS are generally relatively small [60], [61]. In this paper, the dataset size is 432, which are repeatedly measured by 24 medical students. Although the proposed method achieved promising classification results on three different datasets, including the private stress dataset and two public available datasets, with a nested 10-fold cross-validation method, the small sample size may still limit the performance of machine learning methods. Therefore, more data should be collected for future work to alleviate this problem. Third, the proposed method mainly focused on statistical features and potential spatial information of fNIRS signals. Multidimensional information (e.g., temporal, frequency, and spatial connectivity information) could be utilized to detect stress, which will be our future work. Additionally, the experimental paradigm of decision-making used in this study is a computer-mediated interaction. In the future, interaction in real social situations will be considered, which has more ecological effects [62]. What's more, other clinical scenarios (e.g., doctor-patient communication) under stress condition should be further examined to determine whether the JCCB-FSC model is universal in different tasks.

V. CONCLUSION

In this paper, we proposed a novel JCCB-FSC method to detect stress in decision-making. In particular, we used TSST and BART experimental paradigms to simulate the decision-making process of medical students under stress. Different from previous research that focused on simply grading stress in no specific situation, we aimed to detect stress in the decision-making process, and provide clues for stress detection in the decision-making situation of medical staff in the future. In the proposed JCCB-FSC method, regularized regression analysis was used to detect the stress state and select features from the hemodynamic response highly related to stress during decision-making. Different from traditional methods without considering the group structure information of channels and the potential associated information among brain regions, JCCB-FSC considered the potential information of channels and imposed intra- and inter-channel constraints on fNIRS

data to better discover the potential information, and achieved an acceptable stress detection. Overall, the JCCB-FSC would be more flexible in detecting the pressure state and features related to stress in the decision-making process. These findings may guide future efforts to continuously monitor cognitive activity in real life to help improve stress management, thereby reducing the risk of adverse health consequences and decision-making performance caused by stress.

REFERENCES

[1] G. P. Chrousos, "The concepts of stress and stress system disorders: Overview of physical and behavioral homeostasis," *JAMA*, vol. 267, no. 9, p. 1244, Mar. 1992.

[2] P. Morgado, N. Sousa, and J. J. Cerqueira, "The impact of stress in decision making in the context of uncertainty," *J. Neurosci. Res.*, vol. 93, no. 6, pp. 839–847, 2015.

[3] C. J. Groombridge, Y. Kim, A. Maini, D. V. Smit, and M. C. Fitzgerald, "Stress and decision-making in resuscitation: A systematic review," *Resuscitation*, vol. 144, pp. 115–122, Nov. 2019.

[4] V. R. LeBlanc, C. Regehr, W. Tavares, A. K. Scott, R. MacDonald, and K. King, "The impact of stress on paramedic performance during simulated critical events," *Prehospital Disaster Med.*, vol. 27, no. 4, pp. 369–374, Aug. 2012.

[5] A. Harvey, G. Bandiera, A. B. Nathens, and V. R. LeBlanc, "Impact of stress on resident performance in simulated trauma scenarios," *J. Trauma Acute Care Surg.*, vol. 72, no. 2, pp. 497–503, 2012.

[6] C. M. Wetzel *et al.*, "Stress management training for surgeons—A randomized, controlled, intervention study," *Ann. Surg.*, vol. 253, no. 3, pp. 488-494, 2011.

[7] N. E. Anton *et al.*, "Stress and resident interdisciplinary team performance: Results of a pilot trauma simulation program," *Surgery*, vol. 170, no. 4, pp. 1074–1079, 2021.

[8] K. Starcke and M. Brand, "Decision making under stress: A selective review," *Neurosci. Biobehavioral Rev.*, vol. 36, no. 4, pp. 1228–1248, Apr. 2012.

[9] T. K. Liu, Y. P. Chen, Z. Y. Hou, C. C. Wang, and J. H. Chou, "Noninvasive evaluation of mental stress using by a refined rough set technique based on biomedical signals," *Artif. Intell. Med.*, vol. 61, no. 2, pp. 97–103, Jun. 2014.

[10] G. P. Chrousos, "Stress and disorders of the stress system," *Nature Rev. Endocrinol.*, vol. 5, no. 7, pp. 374–381, Jul. 2009.

[11] N. C. Nicolaides, E. Kyratzi, A. Lamprokostopoulou, G. P. Chrousos, and E. Charmandari, "Stress, the stress system and the role of glucocorticoids," *Neuroimmunomodulation*, vol. 22, nos. 1–2, pp. 6–19, 2015.

[12] Q. Yang, Y. Li, D. Sun, and T. M. C. Lee, "The effects of stress on risky and social decision making," *Adv. Psychol. Sci.*, vol. 24, no. 6, p. 974, 2016.

[13] H. Ashton, R. D. Savage, J. W. Thompson, and D. W. Watson, "A method for measuring human behavioural and physiological responses at different stress levels in a driving simulator," *Brit. J. Pharmacol.*, vol. 45, no. 3, pp. 532–545, Jul. 1972.

[14] D. H. Hellhammer, S. Wüst, and B. M. Kudielka, "Salivary cortisol as a biomarker in stress research," *Psychoneuroendocrinology*, vol. 34, no. 2, pp. 163–171, Feb. 2009.

[15] L. G. Douma and M. L. Gumz, "Circadian clock-mediated regulation of blood pressure," *Free Radical Biol. Med.*, vol. 119, pp. 108–114, May 2018.

[16] J. F. Thayer, S. S. Yamamoto, and J. F. Brosschot, "The relationship of autonomic imbalance, heart rate variability and cardiovascular disease risk factors," *Int. J. Cardiol.*, vol. 141, no. 2, pp. 122–131, May 2010.

[17] C. S. H. Ho *et al.*, "Diagnostic and predictive applications of functional near-infrared spectroscopy for major depressive disorder: A systematic review," *Systematic Rev.*, vol. 11, p. 378, May 2020.

[18] Y. Hoshi, "Towards the next generation of near-infrared spectroscopy," *Philos. Trans. Roy. Soc. A, Math., Phys. Eng. Sci.*, vol. 369, no. 1995, pp. 4425–4439, 2011.

[19] J. D. Rieke *et al.*, "Development of a combined, sequential real-time fMRI and fNIRS neurofeedback system to enhance motor learning after stroke," *J. Neurosci. Methods*, vol. 341, Jul. 2020, Art. no. 108719.

[20] D. Rosenbaum *et al.*, "Insights from a laboratory and naturalistic investigation on stress, rumination and frontal brain functioning in MDD: An fNIRS study," *Neurobiol. Stress*, vol. 15, Nov. 2021, Art. no. 100344.

[21] D. Rosenbaum *et al.*, "Stress-related dysfunction of the right inferior frontal cortex in high ruminators: An fNIRS study," *NeuroImage, Clin.*, vol. 18, pp. 510–517, Jan. 2018.

[22] F. Al-shargie, T. B. Tang, and M. Kiguchi, "Mental stress grading based on fNIRS signals," in *Proc. 38th Annu. Int. Conf. IEEE Eng. Med. Biol. Soc. (EMBC)*, Aug. 2016, pp. 5140–5143.

[23] R. Zhang *et al.*, "Effects of acute psychosocial stress on interpersonal cooperation and competition in young women," *Brain Cognition*, vol. 151, Jul. 2021, Art. no. 105738.

[24] A. M. Y. Tai *et al.*, "Machine learning and big data: Implications for disease modeling and therapeutic discovery in psychiatry," *Artif. Intell. Med.*, vol. 99, Aug. 2019, Art. no. 101704.

[25] S. Woo, "Classification of stress and non-stress condition using functional near-infrared spectroscopy," in *Proc. 18th Int. Conf. Control, Autom. Syst. (ICCAS)*, 2018, pp. 1147–1151.

[26] S. Park and S. Y. Dong, "Effects of daily stress in mental state classification," *IEEE Access*, vol. 8, pp. 201360–201370, 2020.

[27] N. Karamzadeh *et al.*, "A machine learning approach to identify functional biomarkers in human prefrontal cortex for individuals with traumatic brain injury using functional near-infrared spectroscopy," *Brain Behav.*, vol. 6, no. 11, p. 541, Nov. 2016.

[28] R. Afridi, S. Seol, H. J. Kang, and K. Suk, "Brain-immune interactions in neuropsychiatric disorders: Lessons from transcriptome studies for molecular targeting," *Biochem. Pharmacol.*, vol. 188, Jun. 2021, Art. no. 114532.

[29] C. Feng *et al.*, "Common brain networks underlying human social interactions: Evidence from large-scale neuroimaging meta-analysis," *Neurosci. Biobehavioral Rev.*, vol. 126, pp. 289–303, Jul. 2021.

[30] S. Çavdar, A. E. Aydın, O. Algın, and S. Aydın, "The complex structure of the anterior white commissure of the human brain: Fiber dissection and tractography study," *World Neurosurgery*, vol. 147, pp. e111–e117, Mar. 2021.

[31] D. Rosenbaum *et al.*, "Cortical hemodynamic changes during the trier social stress test: An fNIRS study," *NeuroImage*, vol. 171, pp. 107–115, May 2018.

[32] C. W. Lejuez *et al.*, "Evaluation of a behavioral measure of risk taking: The balloon analogue risk task (BART)," *J. Exp. Psychol., Appl.*, vol. 8, no. 2, pp. 75–84, 2002.

[33] M. Kim, J. H. Won, J. Youn, and H. Park, "Joint-connectivity-based sparse canonical correlation analysis of imaging genetics for detecting biomarkers of Parkinson's disease," *IEEE Trans. Med. Imag.*, vol. 39, no. 1, pp. 23–34, Jan. 2020.

[34] M. Huang, X. Chen, Y. Yu, H. Lai, and Q. Feng, "Imaging genetics study based on a temporal group sparse regression and additive model for biomarker detection of Alzheimer's disease," *IEEE Trans. Med. Imag.*, vol. 40, no. 5, pp. 1461–1473, May 2021.

[35] T. M. Marteau and H. Bekker, "The development of a six-item short-form of the state scale of the Spielberger state—Trait anxiety inventory (STAI)," *Brit. J. Clin. Psychol.*, vol. 31, no. 3, pp. 301–306, Sep. 1992.

[36] B. C. Leigh, "Peril, chance, adventure: Concepts of risk, alcohol use and risky behavior in young adults," *Addiction*, vol. 94, no. 3, pp. 371–383, Mar. 1999.

[37] N. Naseer and K.-S. Hong, "FNIRS-based brain-computer interfaces: A review," *Front. Hum. Neurosci.*, vol. 9, p. 3, Jan. 2015.

[38] L. J. Garey, *Brodmann's' Localisation in the Cerebral Cortex'*. Singapore: World Scientific, 1999.

[39] H. Peng, F. Long, and C. Ding, "Feature selection based on mutual information criteria of max-dependency, max-relevance, and min-redundancy," *IEEE Trans. Pattern Anal. Mach. Intell.*, vol. 27, no. 8, pp. 1226–1238, Aug. 2005.

[40] J. Chao *et al.*, "FNIRS evidence for distinguishing patients with major depression and healthy controls," *IEEE Trans. Neural Syst. Rehabil. Eng.*, vol. 29, pp. 2211–2221, 2021.

[41] I. Guyon and A. Elisseeff, "An introduction to variable and feature selection," *J. Mach. Learn. Res.*, vol. 3, pp. 1157–1182, Jan. 2003.

[42] M. Cazzell, L. Li, Z.-J. Lin, S. J. Patel, and H. Liu, "Comparison of neural correlates of risk decision making between genders: An exploratory fNIRS study of the balloon analogue risk task (BART)," *NeuroImage*, vol. 62, no. 3, pp. 1896–1911, Sep. 2012.

[43] S. Xu *et al.*, "Differential effects of real versus hypothetical monetary reward magnitude on risk-taking behavior and brain activity," *Sci. Rep.*, vol. 8, no. 1, p. 3712, Dec. 2018.

[44] M. Z. Hasan, M. Z. Hasan, S. M. R. Islam, and S. M. R. Islam, "Suitibility investigation of the different classifiers in fNIRS signal classification," in *Proc. IEEE Region Symp. (TENSYMP)*, Jun. 2020, pp. 1656–1659.
[45] Y. Zhu *et al.*, "Classifying major depressive disorder using fNIRS during motor rehabilitation," *IEEE Trans. Neural Syst. Rehabil. Eng.*, vol. 28, no. 4, pp. 961–969, Apr. 2020.
[46] M. Xia, J. Wang, and Y. He, "BrainNet viewer: A network visualization tool for human brain connectomics," *PLoS ONE*, vol. 8, no. 7, Jul. 2013, Art. no. e68910.
[47] S. U. Maier, A. B. Makwana, and T. A. Hare, "Acute stress impairs self-control in goal-directed choice by altering multiple functional connections within the Brain's decision circuits," *Neuron*, vol. 87, no. 3, pp. 621–631, Aug. 2015.
[48] J. van Oort *et al.*, "How the brain connects in response to acute stress: A review at the human brain systems level," *Neurosci. Biobehavioral Rev.*, vol. 83, pp. 281–297, Dec. 2017.
[49] M. P. Herzberg and M. R. Gunnar, "Early life stress and brain function: Activity and connectivity associated with processing emotion and reward," *NeuroImage*, vol. 209, Apr. 2020, Art. no. 116493.
[50] P. Shang, 2020, "Processed data. V1," Mendeley Data, doi: 10.17632/6mbzffznr6.1.
[51] T. J. Huppert, S. G. Diamond, M. A. Franceschini, and D. A. Boas, "HomER: A review of time-series analysis methods for near-infrared spectroscopy of the brain," *Appl. Opt.*, vol. 48, no. 10, pp. D280–D298, 2009.
[52] X. Li, M. A. Krol, S. Jahani, D. A. Boas, H. Tager-Flusberg, and M. A. Yücel, "Brain correlates of motor complexity during observed and executed actions," *Sci. Rep.*, vol. 10, no. 1, p. 10965, Dec. 2020.
[53] S. Wijeakumar, T. J. Huppert, V. A. Magnotta, A. T. Buss, and J. P. Spencer, "Validating an image-based fNIRS approach with fMRI and a working memory task," *NeuroImage*, vol. 147, pp. 204–218, Feb. 2017.
[54] D. D. de Faria *et al.*, "Task-related brain activity and functional connectivity in upper limb dystonia: A functional magnetic resonance imaging (fMRI) and functional near-infrared spectroscopy (fNIRS) study," *Neurophotonics*, vol. 7, no. 4, pp. 1–13, Oct. 2020.
[55] Z. Wang, J. Zhang, X. Zhang, P. Chen, and B. Wang, "Transformer model for functional near-infrared spectroscopy classification," *IEEE J. Biomed. Health Informat.*, vol. 26, no. 6, pp. 2559–2569, Jun. 2022.
[56] L. D. Godoy, M. T. Rossignoli, P. Delfino-Pereira, N. Garcia-Cairasco, and E. H. de Lima Umeoka, "A comprehensive overview on stress neurobiology: Basic concepts and clinical implications," *Review*, vol. 12, p. 127, Jul. 2018.
[57] P. Morgado, N. Sousa, and J. J. Cerqueira, "The impact of stress in decision making in the context of uncertainty," *J. Neurosci. Res.*, vol. 93, no. 6, pp. 839–847, Jun. 2015.
[58] J. Brunelin and S. Fecteau, "Impact of bifrontal transcranial direct current stimulation on decision-making and stress reactivity. A pilot study," *J. Psychiatric Res.*, vol. 135, pp. 15–19, Mar. 2021.
[59] N. Singer, M. Sommer, S. Wust, and B. M. Kudielka, "Effects of gender and personality on everyday moral decision-making after acute stress exposure," *Psychoneuroendocrinology*, vol. 124, Feb. 2021, Art. no. 105084.
[60] K. S. Button *et al.*, "Power failure: Why small sample size undermines the reliability of neuroscience," *Nature Rev. Neurosci.*, vol. 14, no. 5, pp. 365–376, 2013.
[61] A. Von Lühmann, X. Li, K.-R. Müller, D. A. Boas, and M. A. Yücel, "Improved physiological noise regression in fNIRS: A multimodal extension of the general linear model using temporally embedded canonical correlation analysis," *NeuroImage*, vol. 208, Mar. 2020, Art. no. 116472.
[62] S. Sonkusare, M. Breakspear, and C. Guo, "Naturalistic stimuli in neuroscience: Critically acclaimed," *Trends Cognit. Sci.*, vol. 23, no. 8, pp. 699–714, Aug. 2019.